PLANE STRAIN DEFORMATION NEAR A CRACK TIP IN A POWER LAW HARDENING MATERIAL

J. R. RICE and G. F. ROSENGREN

PLANE STRAIN DEFORMATION NEAR A CRACK TIP

IN A POWER LAW HARDENING MATERIAL

by

J. R. Rice[*] and G. F. Rosengren[**]

Division of Engineering

BROWN UNIVERSITY

Providence, Rhode Island

July 1967

[*] Assistant Professor of Engineering, Brown University, Providence, R. I.

[**] Research Assistant in Engineering, Brown University, Providence, R. I.

Abstract

Crack tip strain singularities are investigated with the aid of an energy line integral exhibiting path independence for all contours surrounding a crack tip in a two dimensional deformation field of an elastic material (or elastic-plastic material treated by a deformation theory). It is argued that the product of stress and strain exhibits a singularity varying inversely with distance from the tip in all materials. Corresponding near crack tip stress and strain fields are obtained for the plane straining of an incompressible elastic-plastic material hardening according to a power law. A noteworthy feature of the solution is the rapid rise of triaxial stress concentration above the flow stress with increasing values of the hardening exponent. Results are presented graphically for a range of hardening exponents, and the interpretation of the solution is aided by a discussion of analogous results in the better understood anti-plane strain case.

Introduction

Elastic-plastic analyses of deformation fields near cracks are of obvious relevance to the mechanics of fracture. Little progress has been made on the important problems of tensile loadings opening a crack, although the anti-plane strain case is now well understood for both perfectly plastic (Hult and McClintock, 1956) and strain hardening (Neuber, 1961; Rice, 1967a) materials, and some useful approximate models (Dugdale, 1960; Rice, 1967b) have been proposed for tensile cases. A recent analytical technique developed by Rice (1967c) identifies a line integral which has the same value for all paths encircling the tip of a crack or flat surfaced notch in two dimensional deformation fields of linear or non-linear elastic materials. Appropriate choices of the integration path have led to approximate estimates of strain concentrations for a variety of notch problems; we here employ the method as a starting point in the analysis of near crack tip deformation fields in the plane straining of materials which harden according to a power law relation between stress and strain.

Let

$$W(\underset{\sim}{\varepsilon}) = \int_0^{\underset{\sim}{\varepsilon}} \sigma_{ij} \, d\varepsilon_{ij}$$

denote the energy density of an elastic material. Then considering a homogeneous body of this material containing a traction free crack and subjected to a two dimensional deformation field (Fig. 1, all stresses depend only on x and y), the line integral

$$J = \int_\Gamma [W(\underset{\sim}{\varepsilon})dy - \underset{\sim}{T} \cdot \frac{\partial \underset{\sim}{u}}{\partial x} \, ds] \tag{1}$$

has the same value for all paths Γ surrounding the tip. Here the path is

traversed in the contra-clockwise sense, $\underset{\sim}{T}$ is the traction vector on Γ defined according to the outward normal, $T_i = \sigma_{ij} n_j$, $\underset{\sim}{u}$ is the displacement vector, and s is arc length. Path independence is readily demonstrated in a standard fashion by choosing two separate integration paths Γ_1 and Γ_2. Since the integrand vanishes on the crack surfaces, $J_2 - J_1$ is the above integral carried around the boundary of the area between Γ_1 and Γ_2, and a Green-Gauss type transformation of a line integral to an area integral immediately leads to $J_2 - J_1 = 0$, proving path independence. As no success has been met in finding similar path independent integrals for incremental elastic-plastic stress strain relations, we are here forced to consider a deformation theory of plasticity which is in reality a non-linear elasticity. In particular, we consider an incompressible material with a relation between deviatoric stresses and strains of the Mises form

$$ s_{ij} = \frac{2\tau}{\gamma} \epsilon_{ij} \qquad (2) $$

where $\tau = \sqrt{\frac{1}{2} s_{ij} s_{ij}}$ and $\gamma = \sqrt{2\epsilon_{ij}\epsilon_{ij}}$ and with the hardening following a power law of the form

$$ \tau = G\gamma = \frac{\tau_o}{\gamma_o} \gamma \quad \text{for} \quad \gamma < \gamma_o $$

$$ (3) $$

$$ \tau = \tau_o \left(\frac{\gamma}{\gamma_o}\right)^N \quad \text{for} \quad \gamma > \gamma_o \ . $$

Here τ_o, γ_o are the yield stress and strain in shear, and N is the hardening exponent. As our concern will be only with the near crack tip strain singularity, incompressibility is not expected to be a poor approximation for moderate strain hardening as plastic strains are incompressible. Also, the resulting near tip solution involves proportional flow so that a

deformation theory is less objectionable than usually the case.

The utility of the path independent integral lies largely in the fact that its value may be simply determined for a variety of cases and configurations (Rice, 1967c). For example, the integral has the same value as for the linear elastic solution to a given problem when the yield zone is small compared to geometric dimensions of the problem. This is because such small scale yielding solutions may be obtained through a boundary layer approach (Rice 1967a,b) in which actual boundary conditions are replaced by the requirement of an asymptotic approach to Irwin's (1960) characteristic linear elastic inverse square root stress distribution at large distances from the tip. An extension of the integration path to infinity then requires that only the asymptotically approached field contributes, and the small scale yielding value of J is

$$J = \frac{(1-\nu^2)K_I^2}{E} \ . \tag{4}$$

Here K_I is Irwin's stress intensity factor, and for the well known problem of a crack of length 2a subjected to a uniform remote tension σ_∞

$$J = \frac{\pi(1-\nu^2)\sigma_\infty^2 a}{E} \ . \tag{5}$$

Approximate evaluations of J for large scale yielding are possible due to the relation of the line integral to the rate of variation of equilibrium potential energy of a cracked body with respect to crack length. One such approximation is given and others are suggested by Rice (1967c).

Crack Tip Singularities

Choosing a circular path of radius r for the evaluation of J, Eq. (1) becomes

$$\frac{J}{r} = \int_{-\pi}^{+\pi} \left\{ W[\underline{\varepsilon}(r,\theta)]\cos\theta - \underline{T}(r,\theta) \cdot \frac{\partial \underline{u}}{\partial x}(r,\theta) \right\} d\theta \qquad (6)$$

Evidently the bracketed integrand $\{...\}$ must exhibit a singularity at the crack tip which, at least in its angular average, depends inversely on distance from the tip. Since all terms within the integrand are of order stress times strain (assuming rotations to be of the same order as strains) one is tempted to conclude that crack problems in all materials result in a $1/r$ singularity in the product of stress and strain,

$$\sigma_{ij}\varepsilon_{ij} \rightarrow \frac{a \text{ function of } \theta}{r} \quad \text{as} \quad r \rightarrow 0 \quad . \qquad (7)$$

While attempts at a rigorous proof of this assertion have not been successful, its validity in solved cases is noteworthy. The inverse square root linear elastic stress singularities are in agreement, as is also an approximate analysis of perfectly plastic plane strain (Rice, 1967c) where a $1/r$ strain singularity results from the centered fan slip line field (Hill, 1950) characteristic of analogous punch problems. Further, the validity of Eq. (7) may be verified in all elastic-plastic anti-plane strain crack solutions (Rice, 1967a).

For power law hardening materials, Eq. (7) implies near crack tip stress and strain distributions of the form

$$\sigma_{ij} \rightarrow r^{-N/(1+N)} \Sigma_{ij}(\theta) \quad , \quad \varepsilon_{ij} \rightarrow r^{-1/(1+N)} E_{ij}(\theta) \qquad (8)$$

Conversely, we may turn our procedure around and prove the following: If stress and strain components have the singular structure of powers of r times functions of θ, then traction free crack surface boundary conditions (which lead directly to path independence) may be satisfied only if the powers

of r are as in Eq. (8). This converse procedure is essentially a concise adaption of Williams' (1957) eigenfunction expansion to the non-linear case, but here we determine the eigenvalue (exponent of r) directly, and have left only the problem of determining the corresponding eigenfunction.

To achieve this latter task, we introduce an Airy stress function U to satisfy equilibrium and give the correct dependence on r:

$$U = \frac{(1+N)^2}{2+N} \; r^{(2+N)/(1+N)} \; f(\theta) \tag{9}$$

Near crack tip stresses are then

$$\sigma_{\theta\theta} = \frac{\partial^2 U}{\partial r^2} = r^{-N/(1+N)} \; f(\theta)$$

$$\sigma_{r\theta} = -\frac{\partial}{\partial r}\left(\frac{1}{r}\frac{\partial U}{\partial \theta}\right) = -\frac{1+N}{2+N} \; r^{-N/(1+N)} \; f'(\theta) \tag{10}$$

$$\sigma_{rr} = \frac{1}{r}\frac{\partial U}{\partial r} + \frac{1}{r^2}\frac{\partial^2 U}{\partial \theta^2}$$

$$= (1+N) \; r^{-N/(1+N)} \; [f(\theta) + \frac{1+N}{2+N} \; f''(\theta)]$$

In a similar fashion, incompressibility and strain compatibility are satisfied by introducing a stream function

$$\Psi = r^{(1+2N)/(1+N)} \; g(\theta) \quad , \tag{11}$$

resulting in displacements

$$U_r = -\frac{1}{r}\frac{\partial \Psi}{\partial \theta} = -r^{N/(1+N)} \; g'(\theta)$$

$$\tag{12}$$

$$U_\theta = \frac{\partial \Psi}{\partial r} = \frac{1+2N}{1+N} \; r^{N/(1+N)} \; g(\theta)$$

Near crack tip strains are

$$\varepsilon_{\theta\theta} = -\varepsilon_{rr} = \frac{N}{1+N} r^{-1/(1+N)} g'(\theta)$$

$$\varepsilon_{r\theta} = -\frac{1}{2} r^{-1/(1+N)} [\frac{1+2N}{(1+N)^2} g(\theta) + g''(\theta)] \tag{13}$$

The functions $f(\theta)$, $g(\theta)$ are not independent, but must be chosen to satisfy the one independent stress-strain relation of Eqs. (2) and the hardening law, Eq. (3), giving the following two equations

$$[f'' + \frac{N(2+N)}{(1+N)^2} f] [g'' + \frac{1+2N}{(1+N)^2} g] = -\frac{4N}{(1+N)^2} g'f'$$

$$[f'' + \frac{N(2+N)}{(1+N)^2} f]^2 + \frac{4}{(1+N)^2} f'^2 \tag{14}$$

$$= \frac{4\tau_o^2}{\gamma_o^{2N}} \cdot \frac{(2+N)^2}{(1+N)^4} \left\{ 4 \frac{N^2}{(1+N)^2} g'^2 + [g'' + \frac{1+2N}{(1+N)^2} g]^2 \right\}^N \ .$$

Solving for $f(\theta)$ from these two equations give, after some algebra, the following fourth order differential equation for f.

$$f^{IV} + \frac{N(2+N)}{(1+N)^2} f'' + \frac{N}{h^2+4Nf'^2} \left\{ \frac{1}{(1+N)^2} [4Nf'' + \frac{1+2N}{1+N} h] [h^2+4f'^2] \right.$$

$$+ \frac{4(1-N)}{(1+N)^2} f'[hh'+4f'f''] + \frac{1-N}{N(1+N)} [3hh'^2+8h'f'f''+4h(f''^2+f'f''')]$$

$$+ \frac{(1-N)(1-3N)}{N^2(1+N)} \cdot \frac{h}{h^2+4f'^2} [hh' + 4f'f'']^2 \right\} = 0 \tag{15}$$

where, for brievety's sake we have put

$$h = (1+N)f'' + \frac{N(2+N)}{1+N} f \qquad (16)$$

Note that the governing differential equation for $f(\theta)$ has an equi-dimensional character, in the sense that if $f(\theta)$ is a solution, then so is any constant times $f(\theta)$. The unknown multiplicative constant is determined in terms of the value J of the path independent integral by inserting our solution into Eq. (6). The equation is solved over the interval $0,\pi$ subject to boundary conditions which insure a solution corresponding to symmetric deformations relative to the crack line. Note that $f(0)$ may be chosen arbitrarily, say as

$$f(0) = 1 \; , \qquad (17)$$

with the solution subject to a later normalization. Symmetry requires that $\sigma_{r\theta}$, $\partial\sigma_{rr}/\partial\theta$, and $\partial\sigma_{\theta\theta}/\partial\theta$ all vanish on $\theta = 0$, leading to two further conditions

$$f'(0) = f'''(0) = 0 \; . \qquad (18)$$

Finally, traction free crack surfaces require $\sigma_{\theta\theta}$ and $\sigma_{r\theta}$ to vanish at $\theta = \pi$, so that

$$f(\pi) = f'(\pi) = 0 \; . \qquad (19)$$

Five boundary conditions appear at first sight to overspecify the fourth order equation for $f(\theta)$. Actually, they do not, for the two conditions at $\theta = \pi$ imply one another. This is because the assumed forms of dependence on r in Eqs. (9, 11) necessarily result in path independence for the integral J and, recalling the proof of path independence sketched out in the introduction, this means that

$$\underset{\sim}{\mathrm{T}}(r,\pi) \cdot \frac{\partial \underset{\sim}{u}}{\partial x}(r,\pi) = -\sigma_{\theta\theta}(r,\pi)\frac{\partial u_\theta(r,\pi)}{\partial r} + \sigma_{r\theta}(r,\pi)\frac{\partial u_r(r,\pi)}{\partial r} = 0 \qquad (20)$$

for all solutions of the equation for $f(\theta)$. Thus the vanishing of $\sigma_{r\theta}$ on the crack surface implies the vanishing of $\sigma_{\theta\theta}$.

Numerical Computations and Graphical Results

For the numerical solution of the differential equation for f, Eq. (15), a fourth order Runge-Kutta integration was used. Since this method can only be used for initial value problems, and ours is a two point problem, as seen from the boundary conditions Eqs. (17), (18) and (19), starting values of $f''(0)$ had to be guessed until two values of $f''(0)$ were found, one giving $f(\pi) < 0$ and the other giving $f(\pi) > 0$, and a linear interpolation procedure could be used. After some trial runs a step size equal to $0.9°$ was found to be a good choice and for all values of N, except for $N \geq 0.9$, rapid convergence was obtained. For $N \geq 0.9$ the solutions were very sensitive to changes in $f''(0)$, reflecting the breakdown of Eq. (15) for $N = 1$, in which case one obtains expressions of the form $0/0$. Consequently, instead of using the interpolation procedure where $N \geq 0.9$, the appropriate interval for $f''(0)$ in these cases was run through by using small increments in $f''(0)$ and the right solution was chosen by inspection of the results.

Because of the complicated form of the differential equation for $f(\theta)$, no attempts have been made to make any error estimates of the numerical calculations. However, since all results for $N = 1$, in which case the analytic solution is easily obtained, are very close to the results for $N = 0.99$, as can be seen from the figures, it is believed that the numerical results can be accepted with great confidence.

In determining the correct multiplicative constant for $f(\theta)$, i.e.

performing the integration of Eq. (6), a 5 point formula was used.

All computations were performed on an IBM-360 and the average computing time for a run was 3.5 min.

In Fig. 2 the power hardening law, Eq. (3), has been drawn for some different values of the hardening exponent N.

From the expressions for the Mises equivalent shear stress τ and shear strain γ one finds

$$\tau = \tau_o \, [R(\theta)/r]^{N/(1+N)} \quad , \quad \gamma = \gamma_o \, [R(\theta)/r]^{1/1+N} \tag{21}$$

where $R(\theta)$ is an expression containing $f(\theta)$ and its derivatives, or, when using the normalized form of $f(\theta)$, $R = R(\theta;J,N)$.

From Eq. (21) one immediately sees that $R(\theta)$ gives the shape of constant equivalent strain lines very near the crack tip and that $R(\theta)$ can be interpreted as an approximate indication of the distance from the crack tip to the elastic-plastic boundary; approximate since our solution gives the singular term only, and not of necessity the complete solution in the plastic region. In Figs. 3 and 4 the nondimensional distance $\gamma_o \tau_o R(\theta)/J$ is shown for different values of N; the latter figure amplifies detail near the crack tip through a twenty five times larger scale. In these figures the extreme closeness between the results for $N = 1$ and 0.99 is readily demonstrated.

In Fig. 5 it is demonstrated how the elastic-plastic boundary in front of and behind the crack tip strongly depends on the hardening exponent. In this figure is also shown how the maximum distance from the crack tip to the elastic-plastic boundary, $\gamma_o \tau_o R_{max}/J$, varies with N.

Using the expressions for the stresses one easily finds that the mean stress, $p = (\sigma_{\theta\theta} + \sigma_{rr})/2$ divided by τ is a function of θ only. Figure 6 shows this θ-variation of p/τ together with the mean stress distribution in the perfectly plastic case, $N = 0$. The latter distribution is easily

obtained from the condition of two regions of constant stress state, one in front and one behind the crack tip, with the regions being built up of isosceles right triangles thus forcing any slip line leaving the crack surface and ending up at the symmetry line in front of the crack tip to swing through an angle of $\pi/2$ giving $p/\tau = 1 + \pi$ at $\theta = 0$ (Hill, 1950 and Rice, 1967c). In this figure again is demonstrated the closeness of the results for $N = 1$ and 0.99 as well as how close the results for $N = 0.005$ and $N = 0$ are to each other.

In Fig. 7 is shown how the ratio of the maximum normal stress to the equivalent stress along the symmetry line ahead of the crack, $\sigma_{\theta\theta}/2\tau \big|_{\theta=0}$, varies with the hardening exponent. The rapid rise over the $1+\pi/2$ value anticipated from perfect plasticity is notable and of interest when, for instance, discussing fracture.

For the displacements one finds, when using the normalized $f(\theta)$, that $u_r \tau_o/J$ and $u_\theta \tau_o/J$ can be expressed as a product of $(r/R)^{N/(1+N)}$ and functions of θ. These normalized displacements were calculated and in Fig. 8 the shape of the deformed crack surfaces in the plastic region are shown for some values of N. An arrow in the figure indicates the displacements at the elastic-plastic boundary behind the crack tip as well as the direction of the displacements at the crack in the plastic region. At the bottom of the figure is also a scale showing the nondimensional distance from the crack tip to the elastic-plastic boundary behind the crack tip, $\gamma_o \tau_o R(\pi)/J$. As seen from the results in Fig. 8, the crack opening is very insensible to the value of the hardening exponent and for $N \leq 0.2$ the crack opening δ_t can be taken to be

$$\delta_t \simeq 0.58 \ J/\tau_o \tag{22}$$

From Fig. 8 one sees also how the blunting of the crack tip varies with N.
However, since our numerical results do not give a clear indication on
whether the distance from the crack tip to the elastic-plastic boundary behind
the crack is zero or not when N = 0 (see Fig. 5), it is not possible to say
anything definite about the deformed shape of the crack surface in that case.
A displacement discontinuity results at the tip according to the slip line
analysis of Rice (1967c).

Finally, Fig. 9 shows how the maximum shear direction varies around the
crack for different N. The straight line segment limit results from the slip
line construction noted earlier for the perfectly plastic case, N = 0. In the
elastic case, N = 1, there is a hydrostatic stress state in front of the
crack thus leaving the maximum shear directions indeterminate for θ = 0. For
all other values of N the maximum shear directions in front of the crack are
in the 45°-directions relative to the symmetry line, and the figure nicely
demonstrates the transition of the distribution of the maximum shear direction
between the two limiting cases, N = 0 and N = 1.

Discussion

We emphasize that our solution gives only the structure of the crack tip
singularity. Thus, for example, predictions of the elastic-plastic boundary
location are approximate. Since the anti-plane strain crack problem (Rice,
1967a) is well understood, some insight into the proper interpretation of our
solution might be obtained through an examination of that case. Anti-plane
stress and strain singularities in the form of Eqs. (8) can be found and,
indeed, the complete solution does reveal a deformation field dominated by
such a singularity near the crack tip. It turns out that for small scale

yielding (the boundary layer approach noted in the introduction), the singular forms of Eqs. (8) give the complete solution in the plastic region. Elastic fields can be found which continue the solution across the elastic-plastic boundary predicted by the singular terms, and which meet the asymptotic boundary conditions. This is a remarkable fact, but it is uncertain (and doubted) that a similar role would be played for small scale yielding by the singularities in plane strain.

For anti-plane yielding on a scale comparable to crack length, the elastic-plastic boundary begins to differ significantly from that predicted by the singular term alone. Also, while mathematically the singularity dominates in the limit as $r \to 0$, one finds for small N that strain magnitudes become excessively large and distances from the tip small before the singular term dominates the complete solution. The limit of such behavior results for perfect plasticity ($N = 0$). Then, while the strain field exhibits a $1/r$ singularity, the distribution in θ changes with remote stress level in the large scale yielding range. No unique singular strain distribution exists. A similar feature undoubtedly results for plane strain; the singular term solution appears (from our figures) to have a unique limit as $N \to 0$ but, in fact, our equations do not have a unique solution for the stream function (Eq. 11) when $N = 0$. Nevertheless, the $1/r$ strain singularity would appear necessitated and our solution gives the correct average (in the sense of the J integral) θ dependence of the strength of this singularity.

The very rapid rise of stress triaxiality with strain hardening exponent (Fig. 6) over the practical range for structural metals, say $N = 0.05$ to 0.3, shows that hardening can elevate stresses not only by increasing the flow stress with increasing strain but also by modifying the stress state. Thus, for example, a low yield strength metal may develop local peak stresses in

front of a crack comparable to or in excess of those for a higher strength metal, simply because lower strength materials tend to exhibit greater hardening exponents. The presence of large tensile stresses ahead of a crack is clearly important for the nucleation of micro-cracks in materials capable of cleavage; they are also important for the promotion of ductile fracture mechanisms involving the large growth and final coalescence of voids. Although the later mechanism may appear strain controlled, perfectly plastic calculations for simple configurations (McClintock and Argon, 1966) show a nearly exponential dependence of the rate of void growth per unit of overall strain on the ratio of mean normal stress to yield stress. The role of strain hardening in slowing void growth and raising strains required for coalescence cannot presently be assessed, so that a direct step from this analysis to a crack extension criterion will require further work. Finite geometry changes at the crack tip also influence the deformation state in separation prone material. For example, analyses in the perfectly plastic case do not lead to large strains directly ahead of the crack unless progressive blunting of the tip is considered (Rice, 1967c). Another complicating feature is the distinction which must be made between strain increments due to load elevation and strain increments due to crack advance in incremental elastic-plastic materials (McClintock and Irwin, 1965). Ductile metals exhibit at least a limited amount of stable crack extension prior to catastrophic fracture. The pertinent question in fracture mechanics is more one as to the prediction of final instability than to the prediction of the initiation of crack extension. While the adequate modelling of fracture remains remote, our present solution should be useful for the further understanding of the effects of yielding and hardening, providing other pertinent features of the problem are kept in mind.

We have learned by private communication that Professor J. W. Hutchinson

is conducting similar work on the structure of crack tip singularities, both in plane strain and plane stress, basing his approach on a direct computer assisted adaption of the Williams eigenvalue technique to the non-linear case. He too finds a $1/r$ variation of stress times strain for both deformation modes. Also, Professor J. L. Swedlow reports that a further analysis of experimentally determined plane stress crack tip deformation fields, with data obtained by Gerberich (1964), tends to support a $1/r$ dependence for the product of stress and strain near a crack tip. Grateful acknowledgement for support of this work is made to the Advanced Research Projects Agency (Contract SD-86 with Brown University), and to the National Science Foundation (facilities grant GP-4825) for the support of computer time.

References

D. S. Dugdale (1960). "Yielding of Steel Sheets Containing Slits," J. Mech. Phys. Sol., vol. 8, pp. 100-104.

W. W. Gerberich (1964). "Plastic Strains and Energy Density in Cracked Plates: I. Experimental Techniques and Results," Exper. Mech., vol. 4, no. 11, pp. 335-344.

R. Hill (1950). The Mathematical Theory of Plasticity, Clarendon Press, Oxford.

J. A. Hult and F. A. McClintock (1956). "Elastic-Plastic Stress and Strain Distributions Around Sharp Notches Under Repeated Shear," Proc. Ninth Int'l. Congr. Appl. Mech., Brussels, vol. 8, pp. 51-58.

G. R. Irwin (1960). "Fracture Mechanics," in Structural Mechanics (eds. Goodier and Hoff), Pergamon Press, New York, pp. 557-591.

F. A. McClintock and A. S. Argon (1966). Mechanical Behavior of Materials, (Chap. 16, Ductile Fracture), Addison Wesley, Reading, Mass.

F. A. McClintock and G. R. Irwin (1965). "Plasticity Aspects of Fracture Mechanics," in Symp. on Fracture Toughness, Amer. Soc. Test. Mat'ls., STP-381, pp. 84-113.

H. Neuber (1961). "Theory of Stress Concentration for Shear Strained Prismatical Bodies with Arbitrary Non-Linear Stress Strain Law," Jour. Appl. Mech., vol. 28, pp. 544-550.

J. R. Rice (1967a). "Stresses Due to a Sharp Notch in a Work Hardening Elastic-Plastic Material Loaded by Longitudinal Shear," Jour. Appl. Mech., vol. 34, pp. 287-298.

_____ (1967b). "The Mechanics of Crack Tip Deformation and Extension by Fatigue," in Symp. on Fatigue Crack Growth, (to appear, 1967), Amer. Soc. Test. Mat'ls., STP-415.

_____ (1967c). "A Path Independent Integral and the Approximate Analysis of Strain Concentration by Notches and Cracks," Brown Univ. ARPA SD-86 Report E39.

M. L. Williams (1957). "On the Stress Distribution at the Base of a Stationary Crack," Jour. Appl. Mech., vol. 24, pp. 109-114.
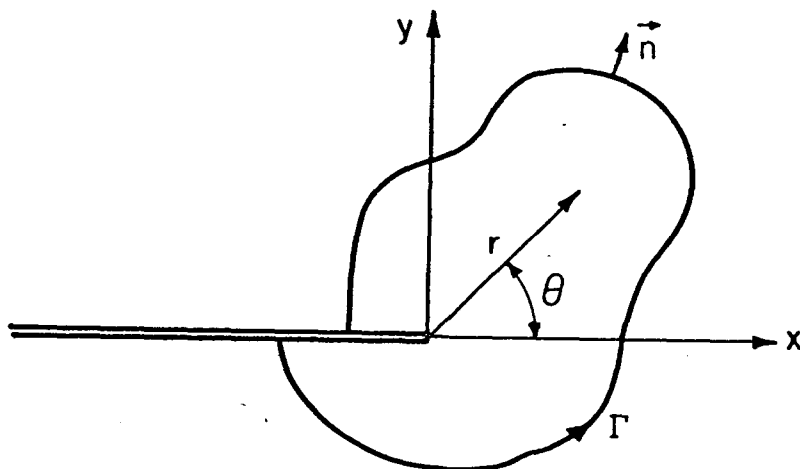
jb

FIG. 1. COORDINATES FOR DESCRIPTION OF CRACK TIP DEFORMATION FIELD, AND
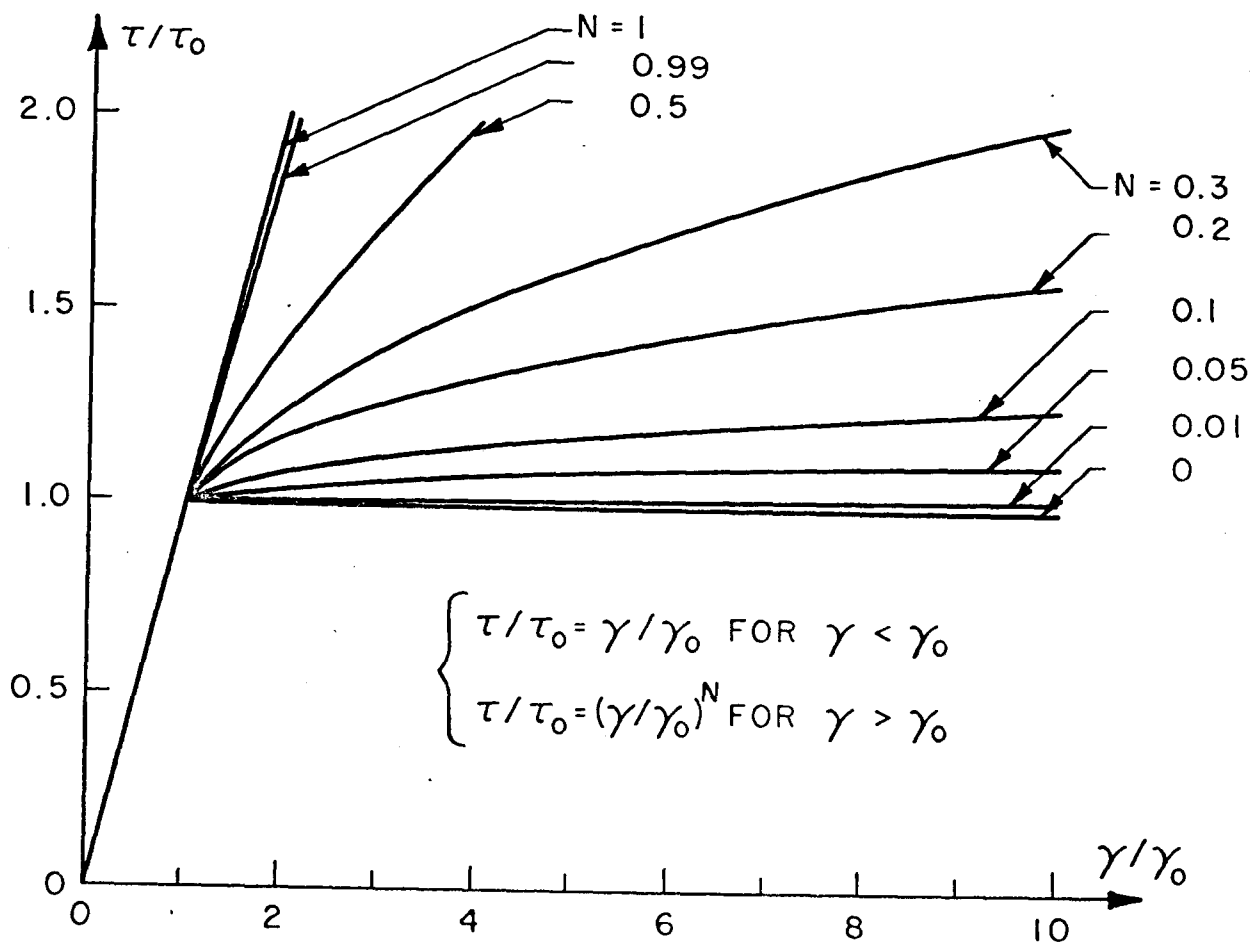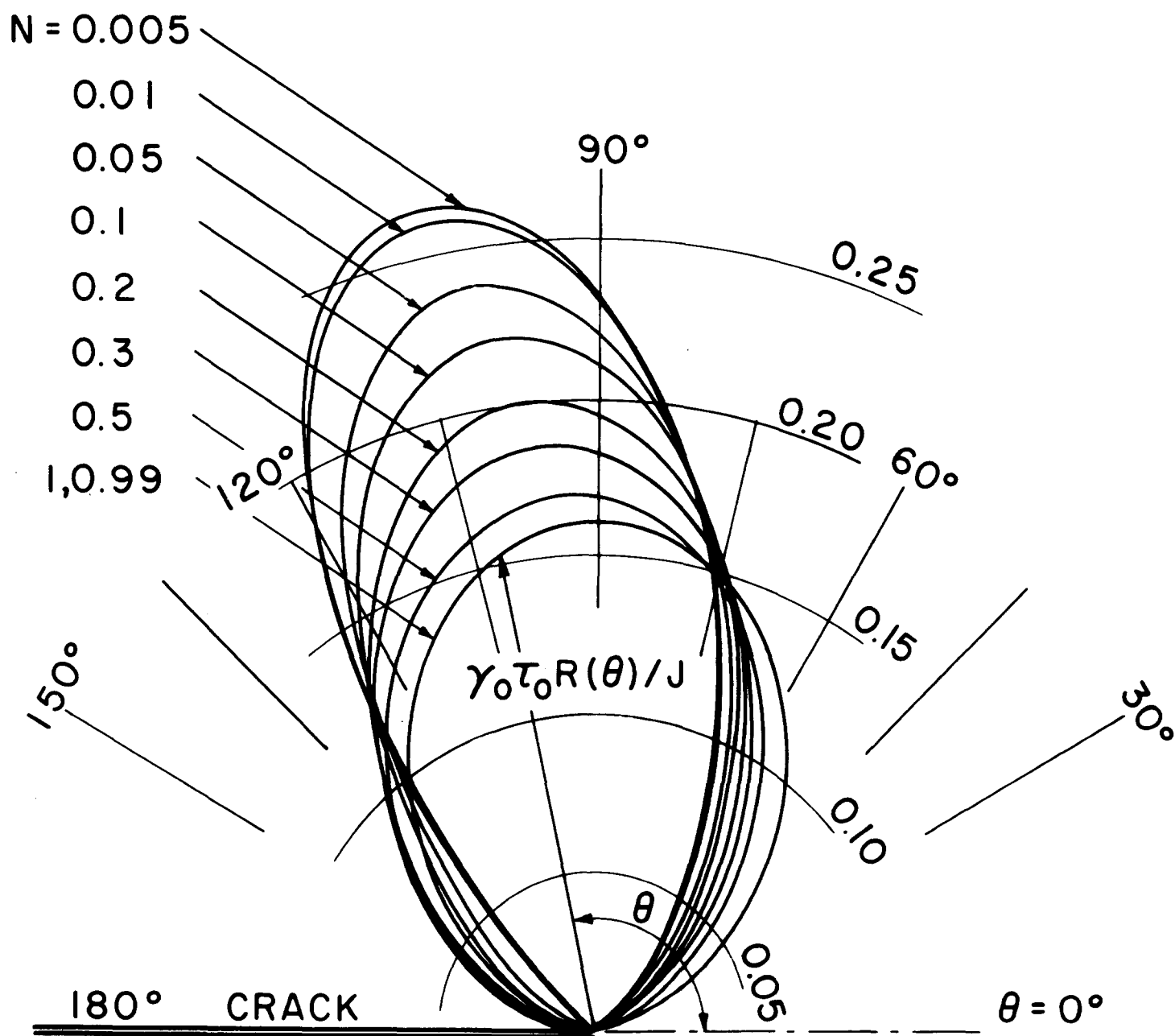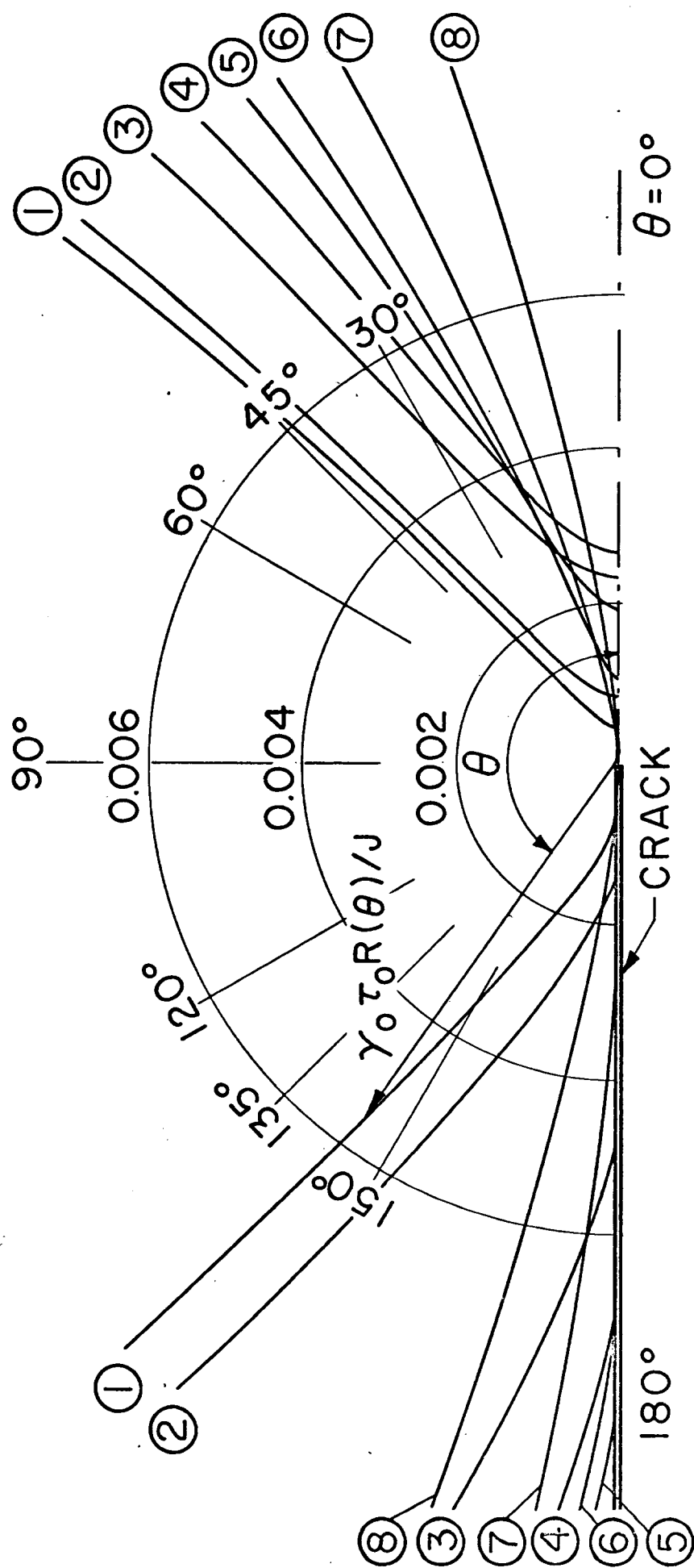TYPICAL CONTOUR Γ FOR EVALUATION OF PATH INDEPENDENT LINE
INTEGRAL.

$$\begin{cases} \tau/\tau_0 = \gamma/\gamma_0 \text{ FOR } \gamma < \gamma_0 \\ \tau/\tau_0 = (\gamma/\gamma_0)^N \text{ FOR } \gamma > \gamma_0 \end{cases}$$

FIG. 2. POWER HARDENING LAW.

N = 0.005
0.01
0.05
0.1
0.2
0.3
0.5
1, 0.99

90°

0.25

0.20   60°

$\gamma_o \tau_o R(\theta)/J$

0.15

120°

150°

30°

0.10

θ

0.05

180°   CRACK

$\theta = 0°$

FIG. 3.   APPROXIMATE LOCATION OF ELASTIC-PLASTIC BOUNDARY AND
GEOMETRICAL SHAPE OF CONSTANT EQUIVALENT SHEAR LINES
VERY NEAR THE CRACK TIP.

FIG. 4. ELASTIC-PLASTIC BOUNDARY; DETAIL VERY NEAR TIP.
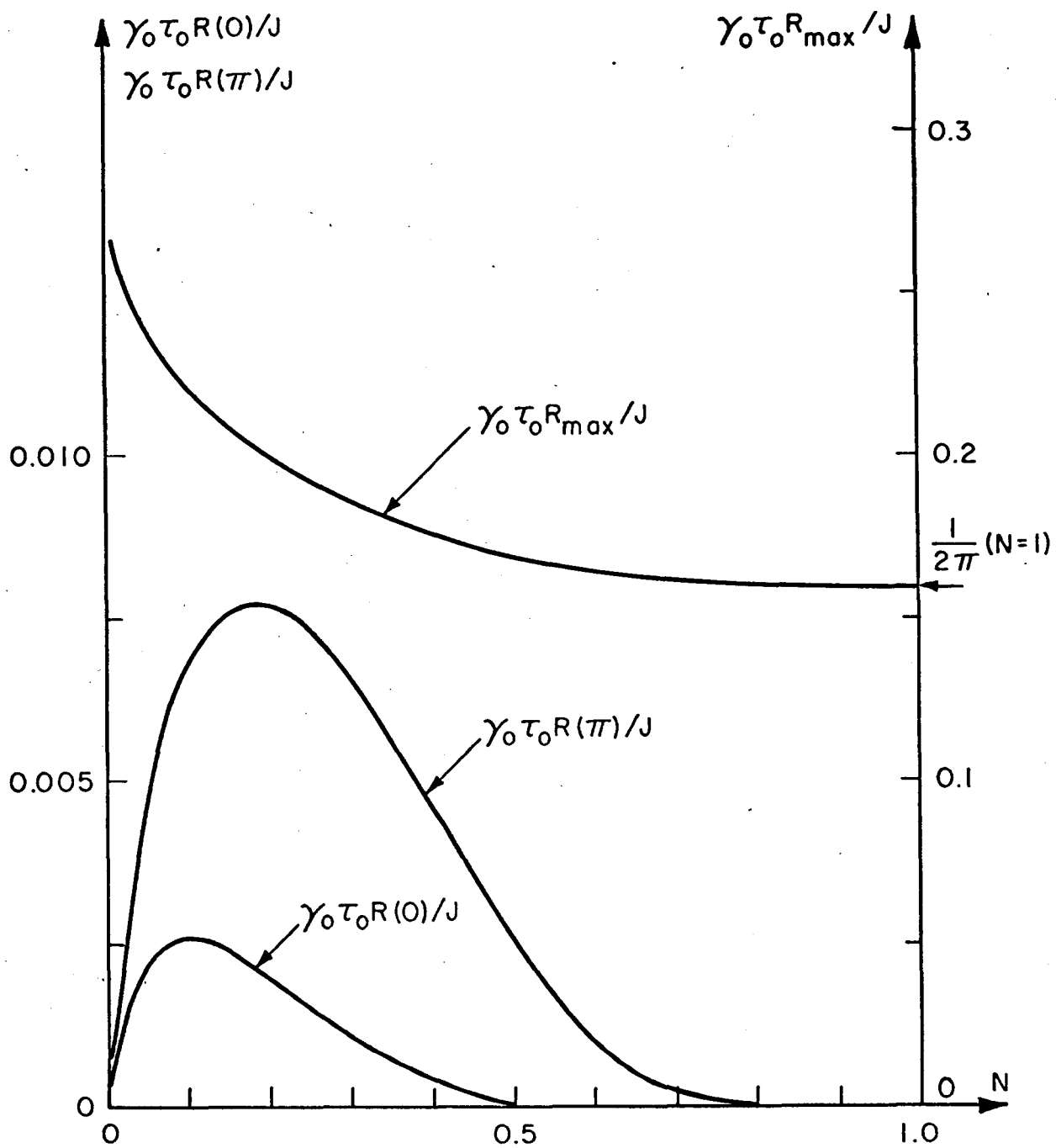
FIG. 5. DISTANCE FROM CRACK TIP TO APPROXIMATE ELASTIC-PLASTIC BOUNDARY
IN FRONT OF AND BEHIND THE CRACK, AS WELL AS MAXIMUM DISTANCE
FROM CRACK TIP TO BOUNDARY.
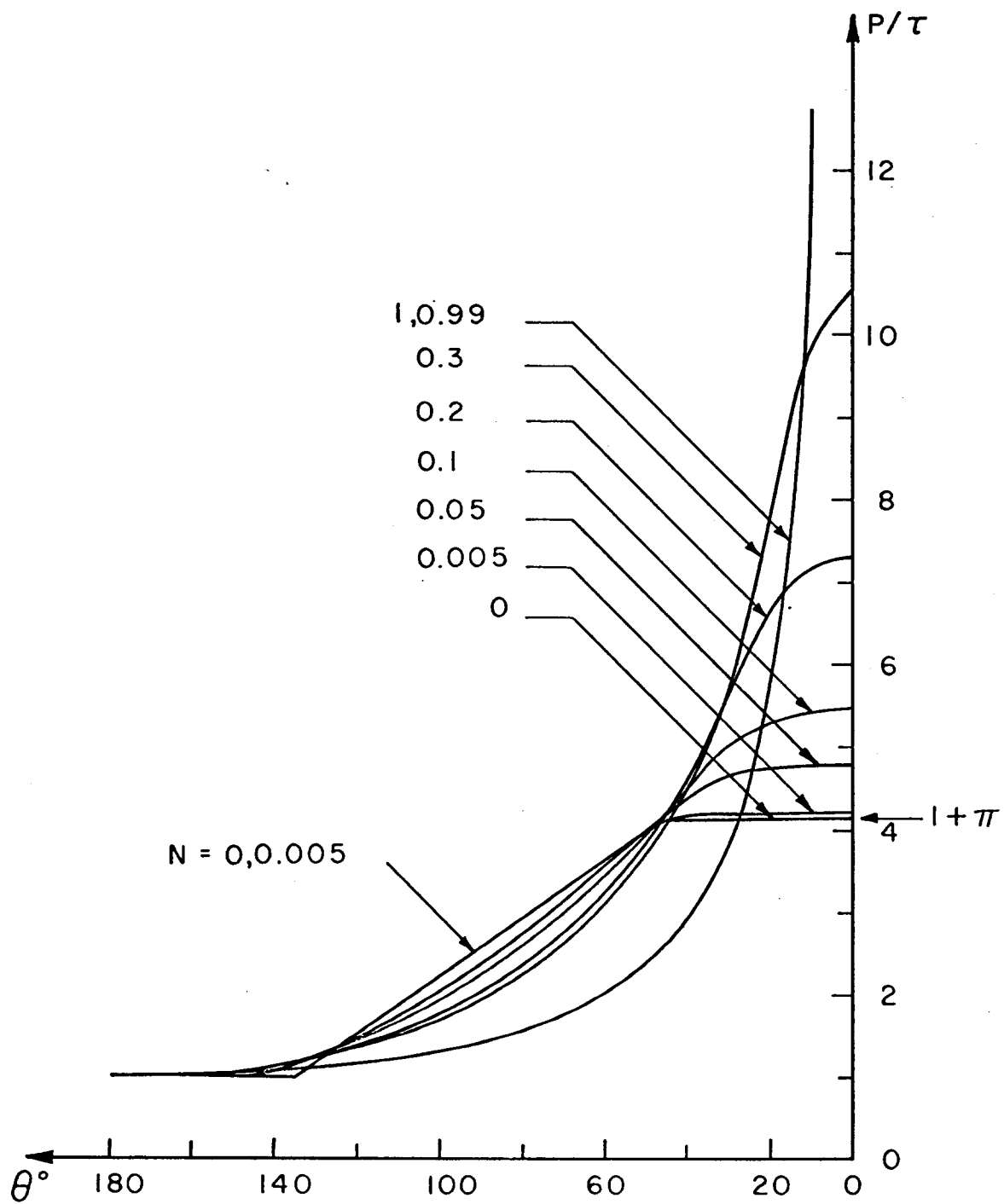
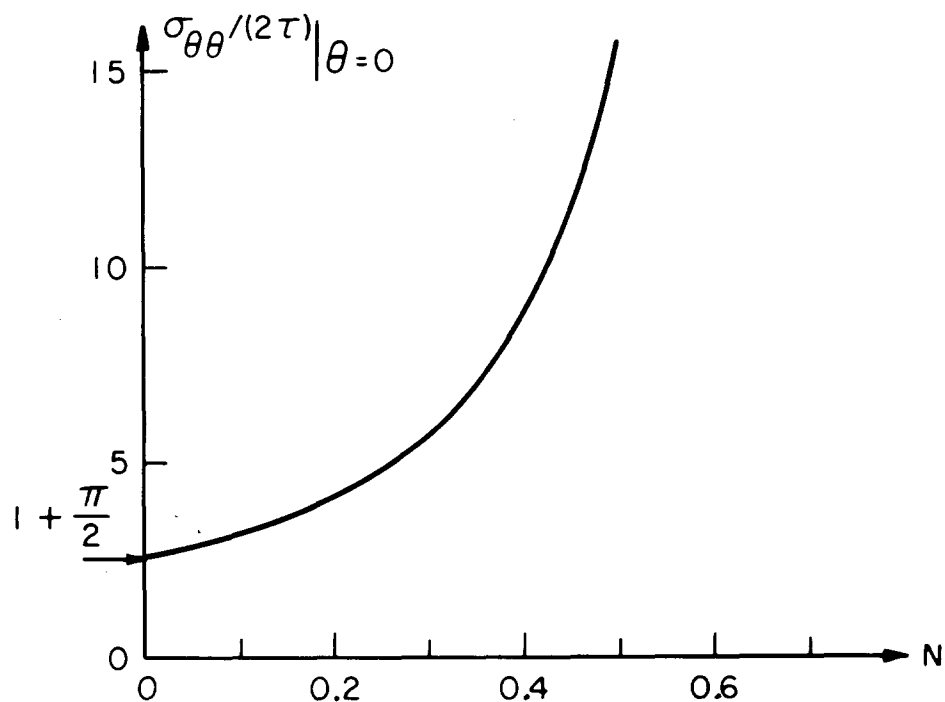FIG. 6. VARIATION OF $p/\tau = (\sigma_{\theta\theta} + \sigma_{rr})/(2\tau)$ WITH θ.

FIG. 7. MAXIMUM NORMAL STRESS TO EQUIVALENT STRESS
FOR $\theta = 0$, $\sigma_{\theta\theta}/2\tau\big|_\theta$, versus N.
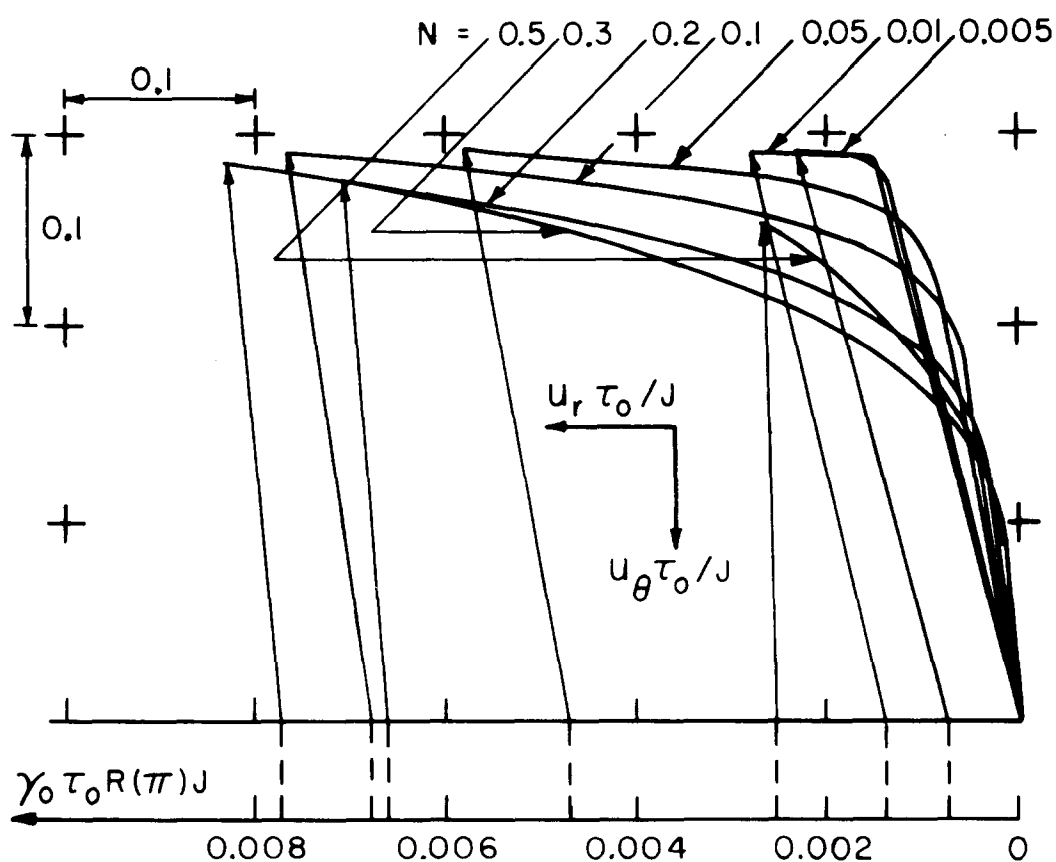

FIG. 8. SHAPE OF DEFORMED CRACK SURFACES IN THE PLASTIC REGION. An arrow
in the figure indicates the displacements at the elastic-plastic
boundary behind the crack tip as well as the direction of the dis-
placements at the crack in the plastic region. The scale at
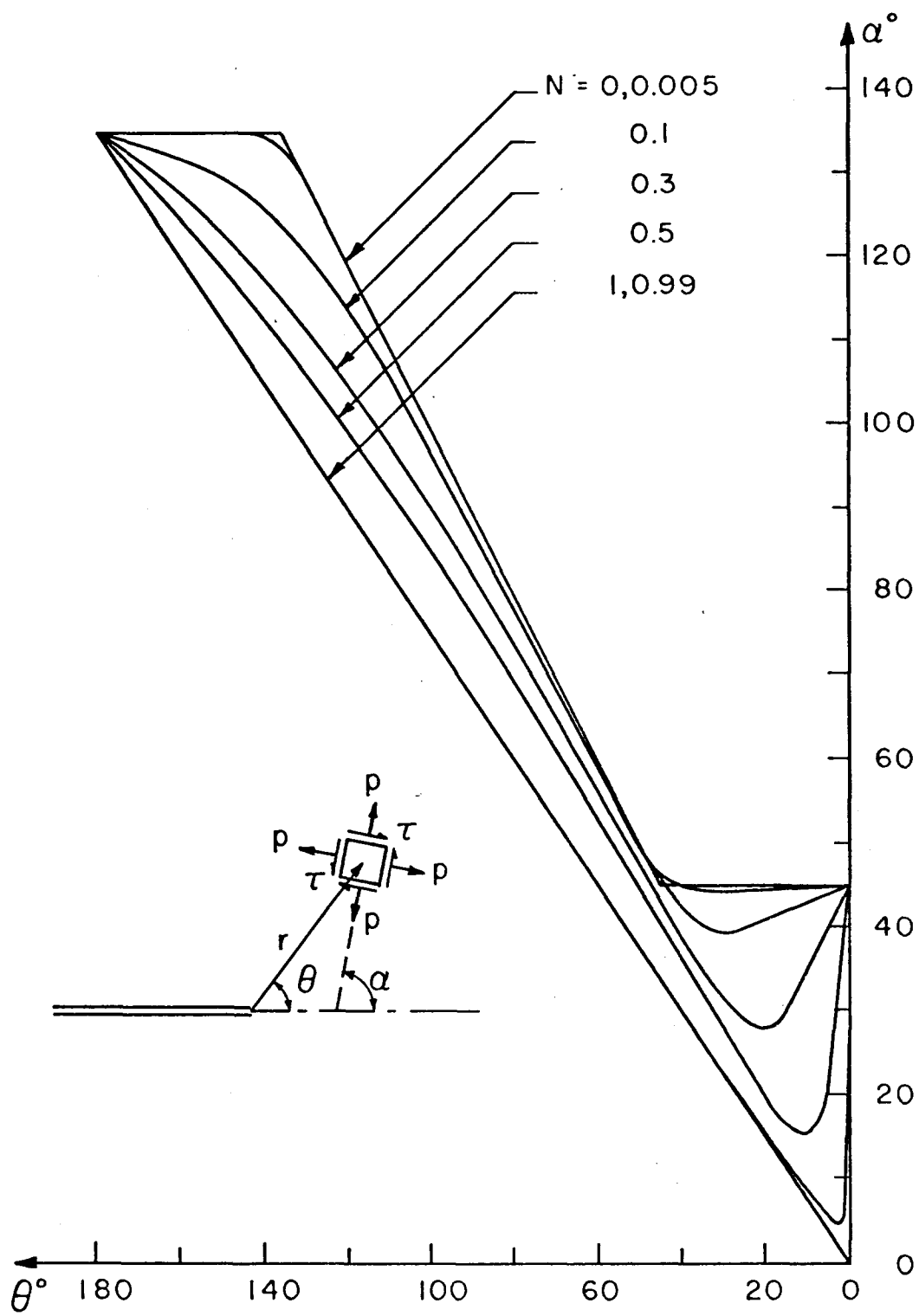bottom of figure shows the nondimensional distance from the crack
tip to the elastic-plastic boundary behind the crack.

FIG. 9. MAXIMUM SHEAR DIRECTIONS.